available at www.sciencedirect.com

ScienceDirect

journal homepage: www.elsevier.com/locate/ecolmodel

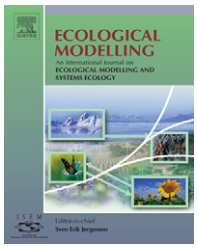

The role of size inequality in self-thinning: A pattern-oriented simulation model for arid savannas

Kerstin Wiegand[a,b,*], *David Saltz*[b,c], *David Ward*[b,d,1], *Simon A. Levin*[a]

[a] *Department of Ecology and Evolutionary Biology, Princeton University, Princeton, NJ 08544, USA*
[b] *Mitrani Department for Desert Ecology, Jacob Blaustein Institute for Desert Research, Ben-Gurion University of the Negev, Sede Boqer 84990, Israel*
[c] *Israel Nature and Parks Authority, 3 Olam vaOlamo Street, 95463 Jerusalem, Israel*
[d] *Ramon Science Center, Jacob Blaustein Institute for Desert Research, Ben-Gurion University of the Negev, Sede Boqer 84990, Israel*

ARTICLE INFO

Article history:
Received 26 April 2006
Received in revised form 5 June 2007
Accepted 15 August 2007
Published on line 30 October 2007

Keywords:
Size inequality
Competitive asymmetry
Zone of influence model
Arid savanna
Acacia reficiens
Namibia
Parsimony
Pattern-oriented modeling

ABSTRACT

The self-thinning line is a very robust pattern, which can be obtained in modeling studies by a variety of different mechanistic assumptions. Our opinion is that we can only advance in our understanding of mechanisms leading to the self-thinning relationship if we demand that the model also reproduces several other characteristic features (patterns) of the self-thinning process such as the degree of size inequality and the average size. We use a pattern-oriented modeling approach to develop a model of self-thinning under size inequality in overcrowded, even-aged stands, which reproduces these three patterns simultaneously. Our approach is to first develop an initial model based on our current ecological knowledge and then to refine the model by modifying the initial model to derive the model that reproduces all patterns of interest.

The initial model is as simple as possible while avoiding incidental, ecologically unjustified, assumptions. It is a further development of zone of influence-simulation models: each plant is described by two circles, one describing a minimum-domain-area and one describing the zone of influence. In the initial model, mortality is "death-by-contact" of minimum-domain-areas and growth is a function of inter-tree competition, i.e. overlapping zones of influence. Model parameterization is based on field data on *Acacia reficiens* in southern Africa. Simulations follow patches of initially small trees through time for up to 1000 years with five parameters, three describing growth and two describing inter-tree competition. A sensitivity analysis shows that all parameters of the initial model contribute significantly to the number and size of plants through time. The two competition parameters, which describe competitive asymmetry and the size of the zone of influence relative to canopy size, are both important for generating size inequality. Thus, both competitive asymmetry and spatial pattern contribute to size inequality, and their relative importance may vary greatly.

The sensitivity analysis suggests that all processes included in the initial model are essential to the evolution of size inequality. However, size inequality under the initial model is

* *Corresponding author*. Present address: Institute of Ecology, University of Jena, Dornburger Str. 159, 07743 Jena, Germany. Tel.: +49 3641 949451; fax: +49 3641 949401.
E-mail address: mail@kerstin-wiegand.de (K. Wiegand).
[1] Present address: School of Biological and Conservation Sciences, University of KwaZulu-Natal, Scottsville 3209, South Africa.
0304-3800/$ – see front matter
doi:10.1016/j.ecolmodel.2007.08.027

below field values, meaning that additional, as yet unconsidered processes, contribute to size inequality. Our best-fit model additionally contains details on growth stochasticity. This study establishes the often-proposed direct link between mortality driven by local competition and self-thinning and highlights the importance of stochasticity in ecological processes.

1. Introduction

Size inequality is a common phenomenon in plants, even in monospecific, even-aged stands (e.g., Hara, 1988). There is controversy regarding whether size inequality is increased by local crowding (meaning that individuals obtain resources depending on the size, proximity, and number of neighbors) or by asymmetry in competition between individuals (meaning that larger individuals obtain a disproportionate share of the resources for their relative size). A series of models (Huston, 1986; Weiner and Thomas, 1986; Miller and Weiner, 1989; Weiner, 1990; Bonan, 1991; Weiner et al., 2001) did not resolve this issue. However, many of these models did not allow for mortality. In this study we focus on size inequality in self-thinning stands.

The well-known self-thinning line relates the (log) mean density of plants to the (log) mean plant size with a slope of −3/2, −4/3, or −2 depending on whether plant size is measured in terms of plant volume, plant biomass, or canopy diameter or diameter at breast height, respectively (Yoda et al., 1963; Enquist et al., 1998; Enquist and Niklas, 2001; Wiegand et al., unpublished). There is some agreement that self-thinning is a local process of resource competition and death of suppressed plants (Hamilton et al., 1995). However, despite a plethora of experimental and theoretical analyses (Westoby, 1984; Hamilton et al., 1995), there is still no agreement about the mechanisms leading to the nearly constant slope of the self-thinning relationship. We argue that this goes back to the fact that the self-thinning line is only one characteristic feature of the self-thinning process (see also Reynolds and Ford, 2005). That different models produce the self-thinning line, indicates that this is a very robust pattern which can easily be reproduced (e.g., Aikman and Watkinson, 1980; Slatkin and Anderson, 1984; Hara, 1985; Adler, 1996; Wiegand et al., unpublished).

The demonstration that a specific mechanism can in theory, generate an observed pattern, is not proof that the mechanism is indeed responsible for that pattern. However, while it may be quite easy to reproduce one characteristic feature of a system, it is not trivial to reproduce several of them simultaneously (Levin, 1992; Kendall et al., 1999; Reynolds and Ford, 1999; Wiegand et al., 2003). This is a basic premise of pattern-oriented modeling (POM) (Wiegand et al., 2003; Grimm et al., 2005). In POM, multiple, characteristic features (hereafter called patterns) are used to (1) optimize model structure, (2) discriminate between alternative hypotheses, and (3) to reduce parameter uncertainty via inverse modeling (Grimm et al., 2005). The basic idea of POM is to compare patterns observed in the field to those generated by several model variants. Aims 1–3 are achieved by searching for the model variant that reproduces the field patterns best. Following the logic of POM, we can only advance in our understanding of mechanisms leading to the self-thinning relationship if the models reproduce several patterns of the system during the self-thinning process simultaneously. For example, the development of size hierarchies in the population can be used as an additional pattern (Hara, 1988; Reynolds and Ford, 2005).

The overarching aim of this study is to improve our understanding of size inequality under self-thinning. We proceed in three steps. First, we develop an individual-based and spatially explicit simulation model (hereafter called "initial model") that summarizes our *a priori* knowledge and hypotheses on self-thinning and size inequality (upper left box in Fig. 1). This model contains, in the simplest way, the leading current hypotheses on self-thinning and size inequality. In POM terminology, the model contains those variables and processes believed to be necessary so that the self-thinning line and size inequality can emerge (Grimm et al., 2005). However, the model is flexible in terms of growth form, the influence of local crowding on resource division among plants, and the degree of competitive asymmetry. As is the case with partially specified models, this flexibility is an attempt to avoid incidental assumptions (Wood, 2001). Model development and parameterization is guided by the case study of *Acacia reficiens* trees in an arid savanna in southern Africa. To gain a more thorough understanding of this model, we explore its behavior via a sensitivity analysis within the entire realistic parameter space. In the second step, we contrast hypotheses on size inequality for the special case of self-thinning populations and find that the hypotheses are not mutually exclusive and interact to generate size inequality ("Basic understanding" in Fig. 1). In the last step, we turn to the specific case of *A. reficiens* and try to quantitatively reproduce three patterns (i.e., the self-thinning line, the degree of size inequality, and the average size of the population at which a certain degree of size inequality is reached) as observed. To make the success of this goal more likely, we use additional variants of the initial model that capture the stochastic nature of plant growth in more detail ("Build refined model variants" in Fig. 1).

2. Site description

Our model is based on a field study in the western edge of the Khomas Hochland, central Namibia, on three adjacent ranches that cover 32,000 ha in total (Wiegand et al., 2005). These ranches are situated between two parallel mountain ranges running north to south. The climate is hot (maximal summer temperatures reach 42 °C) and arid with a distinct, latitude-driven rainfall gradient across the three ranches from 80 mm per annum in the south to 170 mm per annum in the north (Wiegand et al., 2005). Virtually all rain falls in summer (January–April, Ward et al., 2004).

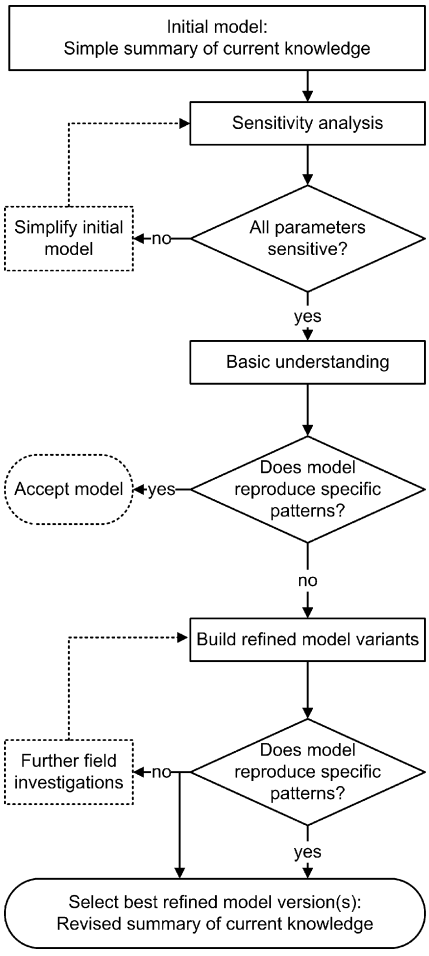

Patterns	Scenarios	Sections	Tab./Fig.
size; Gini	I1-G1 I3-G1	4	E.1/ E.1A,C
G_m; dG_m	I1-G1 I3-G1	5; App. F	-/5
P1; P2	I1-G1	6.1	-/-
P1; P2	I1-G1 I2-G1	6.2	2/6
	G2, G3, G4		
P1; P2	I1-G2; I2-G2 I1-G3: I2-G3 I1-G4: I2-G4	6.2	2/6
	(I2-G4)	6.3	2/6

Fig. 1 – Overview of pattern-oriented modeling procedure employed in this paper including a general flowchart (left half) and details specific to this paper (right hand side). The flowchart shows all steps carried out (solid border lines) and some alternative steps (broken border lines). If the sensitivity analysis would have resulted in non-sensitive parameters, a model simplification would have been necessary. In this paper, all parameters were sensitive and "Basic understanding" refers to the analysis of the two competing hypotheses on the generation on size inequality. If the model would have reproduced the specific patterns, we would have accepted the initial model both as a general representation of the generation of size inequality in plants and a specific model for *A. reficiens* in our Namibian study site. As this was not the case, we built refined model variants. Note that the decision on whether to put rules into the initial model or to reserve them for refined model variants depends on whether these rules may lead to qualitative differences in model behavior (put in initial model) or lead only to quantitative differences in model output (refinements). The last step is to select the refined model version or versions that reproduce all patterns best because this constitutes a summary of the new knowledge on the questions addressed by the model. If patterns are not sufficiently reproduced, appropriate field data should be collected and thereafter a new modeling round attempted. The right hand side of the figure shows the *Patterns* used in each modeling step, the *Scenarios* investigated, the *Section* in which the results are presented and *Tab./Fig.* indicates the tables and figures containing the results. The *horizontal line* indicates whether model parameters were varied globally within the limits given in Table 1 (above the line) or if the standard values given in Table 1 were used (below the line). Note that the patterns used in the modeling procedure proceed from general (here e.g. average tree size) to specific (here e.g. average tree size at which maximum size inequality is reached). General patterns are useful during sensitivity analysis to check if the initial model is in principle able to change these variables. Once this is established, one may proceed to more specific analyses, culminating in quantitative fits of specific patterns. *size*, average minimum-domain-area (in this study equivalent to the plant canopy); *Gini*, size inequality in minimum-domain-areas; G_m, maximum size inequality over the course of an entire simulation; P1, realistic level of maximum size inequality G_m; P2, realistic average minimum-domain-area at which the maximum size inequality is exhibited (dG_m). Note that patterns P1 and P2 are investigated in addition to the self-thinning line (P0). The scenarios differ in initial tree size–frequency distribution and growth. I1, equal sizes; I2, normally distributed sizes; I3, field sizes; G1, initial model; G2, growth rate different among plants but constant through time; G3, stochastic growth rate following a normal distribution with mean *g*; G4, double stochastic growth process accounting for the possibility of both increase (95% probability) and decrease (5%) in plant size as explained in Table 2.

There is a shallow layer of sandy soil overlying Swakop schist from the Damara sequence (Van der Merwe, 1983). Thus, roots of both woody and grassy plants are confined to a thin soil layer (<5–15 cm deep). The vegetation is dry open savanna dominated by *A. reficiens* ("Red thorn" or "False umbrella thorn") with a mixture of *Stipagrostis*, *Eragrostis* and *Entoplocamia* spp. grasses (Ward et al., 2004; Wiegand et al., 2005). *A. reficiens* is a small thorny tree that grows up to 5 m in height in southern Africa, although it seldom reaches above 3 m in our study area (Carr, 1976; Palgrave, 1977; Ross, 1979). As indices of tree size, we use both height (H [m]) and canopy diameter (CD [m]). This is possible because of a strong positive correlation between these two properties in our study site ($\log H = -0.09 + 0.70 \log CD$, $r^2 = 0.93$, $N = 48$ for trees <1.5 m; $\log = \log_{10}$). Strong correlations between these traits have also been recorded in other studies (e.g., Coughenour et al., 1990; Ward and Rohner, 1997).

The spatial distribution of *A. reficiens* in the study area is very patchy. The tree size–frequency distribution within these patches are unimodal or bimodal (presumably representing one or two age-classes, respectively) and are about 50–600 m in extent (Wiegand et al., 2005). Mean tree height is inversely related to tree density with small mean tree heights ($\leqq$0.5 m) at high tree densities ($\geqq$0.5 trees/m) and large mean tree heights (>1.2 m) at low densities (<0.2 trees/m). This pattern can be explained by localized mass germination and subsequent inter-tree competition leading to lower tree densities when trees grow in size (Wiegand et al., 2006).

3. Model description

3.1. General model description

Our initial model simulates the temporal development (growth, mortality) of an even-aged monospecific population of trees distributed in a continuous, square plot, with a basic time step of 5 years. We do not consider reproduction or death due to old age, as we are interested in the dynamics of dense, even-aged, monospecific stands during self-thinning, excluding dynamics outside this frame of interest. Our initial model is a further development of zone of influence (ZOI) models (Bella, 1971; Hara, 1988). In ZOI models, each individual is characterized by its spatial position and a ZOI, representing the area within which the plant has access to resources. ZOI overlap with other plants reduces the growth rate proportional to the overlapped area of ZOIs. In our study area this is probably manifested by competition for water and nutrients. Indeed, an estimate of the size of the ZOI of *A. reficiens* via a fitting procedure based on plant growth with and without competition gave *a posteriori* good agreement between the estimated ZOI of the *Acacia* trees and the maximum extent of the plant's root system (Appendix A in supplementary material). Therefore, we see the ZOI as representing root extent.

As we are interested in self-thinning, our initial model includes – in contrast to most other ZOI models – mortality. To this end, we add a concentric circular minimum-domain-area to our ZOI model. The minimum-domain-area grows proportional to plant size and any overlap with the minimum-domain-areas of neighboring plants leads to the death of the smaller plant. In the case of the canopy-intolerant genus *Acacia* (cf. Smith and Goodman, 1986; Milton, 1995), we see this minimum-domain-area as representing the tree canopy because tree canopies in our study area do virtually not overlap.

3.2. Model scales, instance variables, and output variables

Model scales are characterized by both grain and extent (*sensu* Wiens, 1989). The spatial grain of our initial model is 1 cm, which enables us to adequately describe the location of small individuals. As spatial extent we chose an area of 20 m × 20 m, which balances the disadvantages of many small plants (computational effort) in the early, and few large plants (statistics) in the late, stage of growth and self-thinning. To avoid edge effects, the modeled area is wrapped into a torus (the left and right edges and the top and bottom of the lattice are joined together). In accordance with the slow dynamics of plants in arid environments (e.g., Cody, 2000; Miller and Huenneke, 2000) our model has a temporal grain of 5 years. The temporal extent of 200 simulation steps (1000 years) allows us to follow the development of size inequality under all parameter combinations investigated.

In our initial model, plants are characterized by the following four instance variables:

x: the two-dimensional location of the plant center;
d: a circle of diameter d [cm] centered about x and representing the minimum-domain-area;
ZOI: a circle of diameter $d \times ZOI\_scale$ centered about x. Assuming isometry, we keep the ratio between the ZOI diameter and the minimum-domain-diameter constant at ZOI_scale ($ZOI\_scale > 1$). The choice of ZOI_scale determines the influence of local crowding on resource division. The greater the ZOI_scale, the more plants may compete with each other; and
ZOI_p: the proportion of resources captured from within the ZOI. In the absence of competition, $ZOI_p = 1.0$.

In this study, we represent plants by their two-dimensional minimum-domain-area and ZOI and do not consider biomass. (We can estimate biomass (AB) from canopy diameter (CD) using $\log AB = 2.56 \log CD + 2.82$; Wiegand et al., unpublished.) Our comparisons to field data are also on the basis of a horizontal measure of tree size—namely canopy diameter. This approach better clarifies the mechanisms underlying plant competition by simplifying plant competition into a two-dimensional process, namely gaining as much horizontal spread of roots and shoots as possible. This simplification is reasonable for monospecific even-aged stands where the vertical spread of plants is closely related to horizontal measures of plant size via allometric relationships (Niklas, 1994). While allometry may change due to morphological plasticity in response to competition in several species (Reynolds and Ford, 2005), in absence of evidence for morphological plasticity in *A. reficiens*, we keep our model simple and do not include this possibility.

Model output includes the number of trees in a simulation, their average size, and their size–frequency distribution

at each of the 201 time steps. Inequality in tree size is measured using the Gini coefficient, a non-parametric measure of variation (Glasser, 1962; Weiner and Solbrig, 1984). The Gini coefficient is the average of the absolute differences of all pairs of values in a population divided by twice the average. The coefficient equals 0 when all trees are in the same size class and is 1 when all but one individual is in the smallest size class.

3.3. *Competition*

The competition routine is the heart of the initial model with respect to size inequality. It combines the two leading current hypotheses on the generation of size inequality. One hypothesis is that due to local variation in the size, proximity, and number of neighbors, different plants have access to different quantities of resources and thus size inequality is augmented via differences in their growth rate (Huston, 1986; Miller and Weiner, 1989; Bonan, 1991). This hypothesis is incorporated by means of the ZOI. Specifically, the level of overlap between neighboring plants determines the sharing of resources. Overlap between ZOIs was determined based on Virtual Adaptive Grids (VAGs) approximating the ZOIs (Fig. 2). Each VAG consisted of 20×20 cells and the centers of these cells were the sampling points at which the overlapping neighbors are determined. Details are given in Appendix B.

We divided the overlapping areas among the competitors based on the size asymmetry of competition, i.e. the degree of dominance of big individuals over smaller ones. This is closely related to the second hypothesis, claiming that size variability increases because larger individuals obtain a disproportionate share of the resources for their relative size (Weiner and Thomas, 1986; Weiner, 1990). By this mechanism, initially small difference in plant size will be augmented over time.

Common (restrictive) choices of competitive asymmetry are: (1) complete size asymmetry, i.e. the larger individual obtains all the resources in the area of overlap, and (2) size symmetry, i.e. equal division of the resources within the area of overlap independent of the relative sizes of the competing plants (Hara, 1988; Weiner et al., 2001). We chose not to set the degree of size asymmetry *a priori* and instead use a parameter (b, see Eq. (1)) describing the degree of competitive size asymmetry. If $b = 0$, resources in the VAG cell are divided equally among all competitors and competitive asymmetry increases with increasing b.

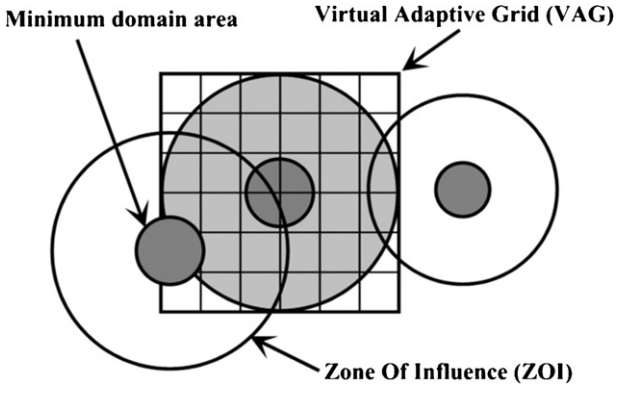

Fig. 2 – Three trees represented by their minimum-domain-area and zone of influence (ZOI). The diameter of the ZOI is *ZOI_scale* (>1) times larger than the diameter of the minimum-domain-area. The Virtual Adaptive Grid (VAG) is used to estimate the degree of overlap among ZOIs of several plants. The scale of this figure is arbitrary as both the ZOI and the VAG scale with the minimum-domain-area.

Both hypotheses influence the proportion of resources captured by each plant, ZOI_p. Technically, ZOI_p is calculated consecutively, plant by plant. For each cell of the VAG covered by the focal plant, all neighbors are identified whose ZOIs cover that cell as well (Fig. 2). The information on the size of these neighbors is used to determine the fraction C_i ($C_i \in [0, 1]$) of resources (area) the focal tree extracts from cell i using a formula based on models by Bella (1971) and Wyszomirski (1992). If the focal tree with $ZOI = ZOI_{focal}$ competes in cell i with j neighbors with ZOIs indexed $ZOI_1, \ldots, ZOI_j$, then the proportion C_i of resources going to the focal tree is given by:

$$C_i = \frac{ZOI_{focal}^b}{ZOI_{focal}^b + \sum_{k=1}^{j} ZOI_{n_k}^b} \quad (1)$$

Finally, the ZOI_p is calculated by adding up the resources conquered from all cells of the VAG of the focal plant (Appendix C).

3.4. *Mortality*

Mortality in the models stems from two sources that act concurrently:

Death-by-contact—As a simple, yet biologically realistic way of modeling mortality in dense stands, we choose "death-by-contact": if the canopies of two plants overlap, the smaller plant dies. This approach is based on the field observations that the smallest individuals have the lowest rate of survivorship (e.g., Ford, 1975; Cannell et al., 1984; Kenkel et al., 1997), the canopies of neighboring *A. reficiens*' rarely overlap, and mortality in encroached *A. reficiens* 10 m × 10 m plots monitored for 5 years was high (Wiegand et al., 2005) while growth was extremely slow (cf. Section 3.8). The latter observation indicates mortality is the dominant space-creating process in this species and, if present, growth plasticity leading to mutual avoidance (Reynolds and Ford, 2005) seems unable to prevent mortality in the long run (5 years and more) and can, therefore, be ignored in a model using basic time steps of 5 years. The death-by-contact rule is key to generating the slope of the self-thinning line (Wiegand et al., unpublished).
Death-by-suppression—To avoid artificial constellations in which small plants are severely suppressed by large plants yet escape death-by-contact because the small plants hide in small gaps among large plants, trees die if they have access to less than a very small proportion, say 1%, of the resources within their ZOI ($ZOI_p < 0.01$). This "death-by-suppression" condition reflects the fact that plants die if they have virtually no access to resources over a long time (note that low ZOI_p values develop slowly through faster growth of neighboring

plants). Although effectively similar, this is different from the rule that plants die when they do not grow, commonly used in simulation models of plants in temperate climates. The absence of growth for several years is common in desert perennials (cf. Goldberg and Turner, 1986; Cody, 2000; Miller and Huenneke, 2000). Our initial model simulates average growth behavior and does not take into account stochastic deviations from average growth. In other words, intermittence of growth for several years and sudden growth boosts are ignored in the initial model (but see rules G2–G4 in Section 3.5).

3.5. Growth

Little is known about height or diameter growth of savanna trees. According to K. Maze and W.J. Bond (cited in Higgins et al., 2000), savanna stems initially grow rapidly in height but growth subsequently slows. For other species, a common choice to model tree growth is the use of logistic-like functions (e.g., Aikman and Watkinson, 1980; Leps and Kindlman, 1987; Bonan, 1988; Davie, 1999). In the initial model, we used a deterministic function of plant size d and competition ZOI_p with neighboring plants based on the generalized logistic equation:

$$d_{t+1} = d_t + d_t \left(1 - \left(\frac{d_t}{d_{\max}}\right)^{\theta}\right) g\, ZOI_p \quad (2)$$

where d_t is the minimum-domain-diameter or, more specifically, the canopy diameter at time t, $d_{\max}$ the maximum attainable canopy diameter attainable, θ influences the shape of the growth curve (influencing the location of the single maximum of the growth increment), and g is the growth rate (Richards, 1959; Gilpin et al., 1976). Note that the proportion of resources captured, ZOI_p takes values between zero and one. Therefore, $g\, ZOI_p$ is an effective growth rate smaller than g due to competition with neighbors.

Stochastic variation of growth is one of the sources of size inequality in even-aged stands (Benjamin and Hardwick, 1986) that may be needed to quantitatively reproduce size inequality. Thus, we investigate four (G1–G4) variations of the growth regime:

(G1) Deterministic growth as described above; used in the initial model.
(G2) Growth rates g constant through time, drawn for each plant at the beginning of the simulation runs from a normal distribution with mean $g = 2.76$ cm/5 years and standard deviation $0.25g$.
(G3) Growth rates g variable in time and among plants, following a normal distribution with mean $g = 2.76$ cm/5 years and standard deviation $0.25g$.
(G4) For savanna trees, a more realistic scenario is one that accounts for both increase and decrease in tree size. Tree size can decrease because of partial dieback of trees due to water stress or trampling and browsing of large animals. This was especially true in the present study where tree size was measured in terms of maximum canopy diameter, a measure sometimes dominated by one branch dying back due to trampling or drought. Thus, we also investigated scenarios in which plant size decreases with a probability of 5%. In each time step, for each plant, it was randomly decided if plant size would increase or decrease and then the growth rate was drawn from normal distributions. In accordance with rules G2 and G3, the standard deviation was set to $0.25g$. In order to conserve the overall mean growth rate g, mean growth rate of shrinking plants was $-g$ while average growth rate of growing plants was set to $2.105g$.

3.6. Initial plant distribution

Variation in post-emergence size is a further source of size inequality in even-aged stands (Benjamin and Hardwick, 1986) that may be needed to quantitatively reproduce size inequality. Thus, we use three types of plant size–frequency distributions to initialize simulations:

(I1) As a null model and to investigate the ability of a model to create size inequality, we started each simulation with all plants being of equal size (mean: 5 cm, e.g., Fig. 3a).
(I2) As a simple way to reflect post-emergence size variability, we distributed initial sizes using a truncated normal distribution (mean: 5 cm, standard deviation 0.25×5 cm = 1.25 cm, distribution tails cut off at 1 cm and 9 cm).
(I3) To initialize simulations with realistic size distributions, we initialize tree sizes with size distributions observed at our field site (e.g., Fig. 3b; for size frequency distributions see Fig. A.1 in supplementary material and for field data collection, see Wiegand et al., 2005).

For all types of size–frequency distributions, the procedures for distributing the plants in space are based on a marked point process invented by Matérn (1960; Appendix D).

3.7. Simulation procedure

All model simulations consisted of several runs (three, if not stated otherwise). Such a small number of replicates is sufficient because all rules of the initial model are deterministic and only the initial spatial distribution of the plants introduces stochasticity. During our attempts to quantitatively reproduce size inequality under self-thinning as observed for *A. reficiens* in Namibia, we conducted simulation experiments with growth rules G2, G3, and G4. In these cases, we increased the number of replicates to 10. In each simulation run, the initial size and location of the trees is determined (see Section 3.6) and, in each of 200 simulation steps, the trees compete with each other, may die, and if they survive, grow. Due to the discrete time step of the model, we had to make a technical decision about the influence of dying trees on competitors in the year of death. Trees dying due to death-by-contact do not have a competitive effect on their neighbors. However, the competitive effect of trees dying due to a low ZOI_p is considered in their year of death. Note that the competitive effect of these trees is very small by definition. We do not consider reproduction because we are interested in the dynamics of even-aged, monospecific, stands after germination. For example, in Namibia, germination of younger *A. reficiens* is prevented by the rarity of rainfall sufficient for

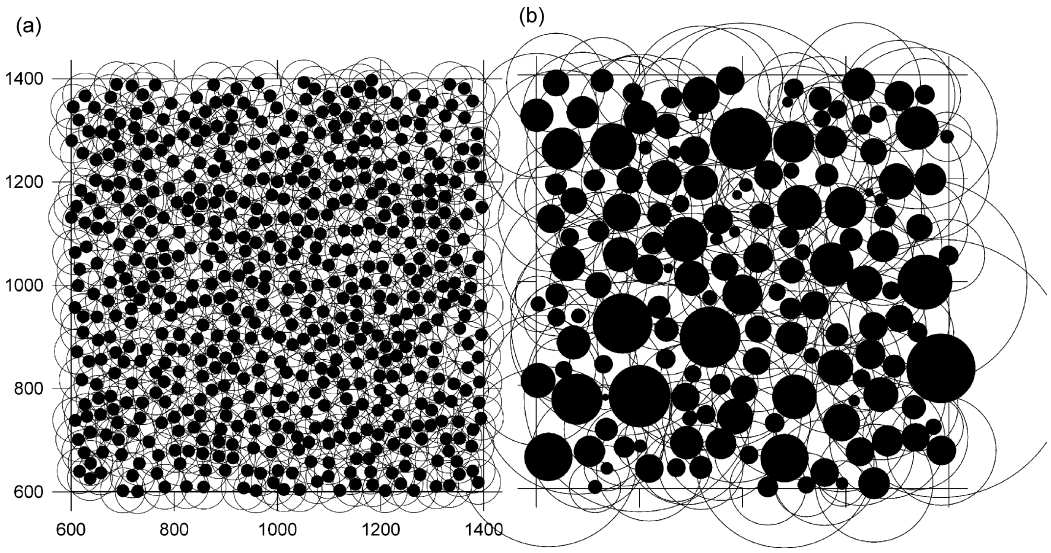

Fig. 3 – Details of spatial plant distributions used to initialize model simulations. Solid discs represent the minimum-domain-area (in this study equivalent to the plant canopy) and open circles the extent of the ZOI. The details (a and b) are 8 m × 8 m in size. (a) All plants are 23.5 cm in canopy diameter. The distribution was generated applying a marked point Matérn process to 16,000 trees in an area of 20 m × 20 m of which 3469 trees remained. This example has been used to estimate the parameter *ZOI_scale* (cf. Section 3.8). (b) Plant sizes follow trees observed in the field in the 10 m × 10 m plot with the smallest average size and greatest number of trees.

germination in arid savannas and the canopy intolerance of Acacias (Wiegand et al., 2006).

To gain a thorough understanding of this model, we first analyze the initial model and explore its behavior via a global sensitivity analysis (Fig. 1). To understand both the ability to generate size inequality and the effect of pre-existing size inequality, simulations are initialized either with trees of equal size (I1) or field sizes (I3). In the second step, we re-analyze simulations from the first step, to investigate how differences in spatial pattern and mode of competition affect size inequality ("Basic understanding" in Fig. 1). Our results will show that all model parameters significantly contribute to average size and size inequality of the plants. Thus, none of the two leading hypotheses for generation of size inequality can be discounted and our initial model appears as a minimum set of rules needed to reproduce size inequality quantitatively. In our third step, we attempt, in addition to reproducing the self-thinning line, to find a model variant that quantitatively meets the patterns "degree of size inequality" and "average plant size at which a certain degree of size inequality is reached" (formally defined in Section 6). As we cannot simplify the initial model, we expand it by testing increasingly realistic growth scenarios (G2–G4; "refined model variants" in Fig. 1) and initial plant size–frequency distributions (I1, I2). Size–frequency distributions observed in the field (I3) are not used in this last step because these plants are relatively large (cf. Fig. 3b).

3.8. *Indirect parameter estimation*

We determined the five parameters in the initial model (Table 1) indirectly by comparing model output to field data on *A. reficiens* in Namibia described in Appendix A and Wiegand et al. (2005). Here we give a brief summary of how we estimated these parameters; details are given in Appendix A. Via a POM approach, *ZOI_scale* was estimated at 3.5 by imitating growth of single trees in a competition experiment. Simulations were run with and without competition under different values of *ZOI_scale*. The underlying idea is that if *ZOI_scale* is, say, too small, competing model trees grow bigger than field trees even though trees that grow alone (without competition) grow to the same size in both the model and the field.

Table 1 – Summary of parameters of the initial model

Parameter	Standard value	Description	Lower limit	Upper limit
θ	0.03	Inflection point of logistic equation	0.01	0.15
g (cm)	2.76	Growth increment in 5 years	0.50	5.00
ZOI_scale	3.5	Diameter ratio ZOI: minimum-domain-area	2.0	5.0
d_{max} (cm)	500	Maximum attainable minimum-domain-area	400	700
b	1.0	Competitive asymmetry	0.0	3.0

Notes: The standard value refers to *Acacia reficiens* in Namibia and the lower and upper limit are limits within which parameters have been varied in the sensitivity analysis. The minimum-domain-area of *A. reficiens* increases with plant growth and corresponds to its canopy.

At this stage of our analysis, we could not estimate competitive asymmetry b from our field data. Consequently, we ran all simulations under several values of b. Maximum attainable canopy diameter d_{max} was estimated at 5 m from the largest trees found outside ephemeral riverbeds and washes at our study site. Again in a POM approach, the growth rate g and the inflection point of the logistic equation θ were estimated concurrently by imitating tree growth as observed in six tree-encroached 10 m × 10 m plots, with a simple non-spatial growth simulation program. Simulations were initialized with the trees observed in the plots and g and θ were accepted when the resulting size–frequency distributions for all plots were not significantly different from the final size–frequency distributions observed in the field. This was the case at $g = 2.76$ cm/5 years and $\theta = 0.03$. Thus, *A. reficiens* trees grow very slowly and growth does not follow the familiar logistic model but rather the Gompertz curve (Eq. (E.1) in supplementary material). Given that we do not have extensive field data, these parameter estimates are approximations only. A global sensitivity analysis of all model parameters is presented in Section 4 and Appendix E.

4. Sensitivity analyses of the initial model

As our model is meant to be applied to a range of locations over which parameter values are changing (e.g., Luxmoore et al., 1991), and because the values of the input parameters are uncertain (e.g., Porco and Blower, 1998), we conducted a global sensitivity analysis. For each time step, we investigated the influence of our five parameters on average tree size and size inequality over time under our initial model. Wiegand et al. (unpublished) show that the initial model reproduces the self-thinning line (see also Fig. 4A). Due to the self-thinning relationship, the influence of the parameters on number of trees present follows directly from the results on average tree size. The sensitivity analysis consisted of 36 parameter combinations well distributed within the entire parameter space given in Table 1 using a stratified sampling method without replacement (Latin hypercube, McKay et al., 2000). Given our focus on self-thinning populations clearly below maximum tree size (and thus mortality due to old age), for each time step, we restricted our analysis to simulations in which the average tree size, averaged over all three simulation runs, was below $0.8d_{max}$. These simulation results were then analyzed for all time steps with linear regression analyses (forward stepwise and multiple linear).

The results of the sensitivity analysis are presented and discussed in detail in Appendix E. In summary, average tree size was well explained (always $r^2 > 0.65$) by the model parameters. The three growth parameters (θ, g, d_{max}) and the competitive asymmetry b had a positive influence on average tree size, while a greater *ZOI_scale* led to slower growth. These contributions were significant, except for d_{max} in simulations initialized with trees of equal size (I1). The contribution of competitive asymmetry b is more significant in simulations initialized with field sizes (I3; $P < 0.05$ vs. <0.001) meaning that b is more important when size inequalities are present. As one would expect, the growth parameters θ and g are also highly significant ($P \leq 0.001$) for the temporal development of average tree size, irrespective of initial tree size–frequency distribution.

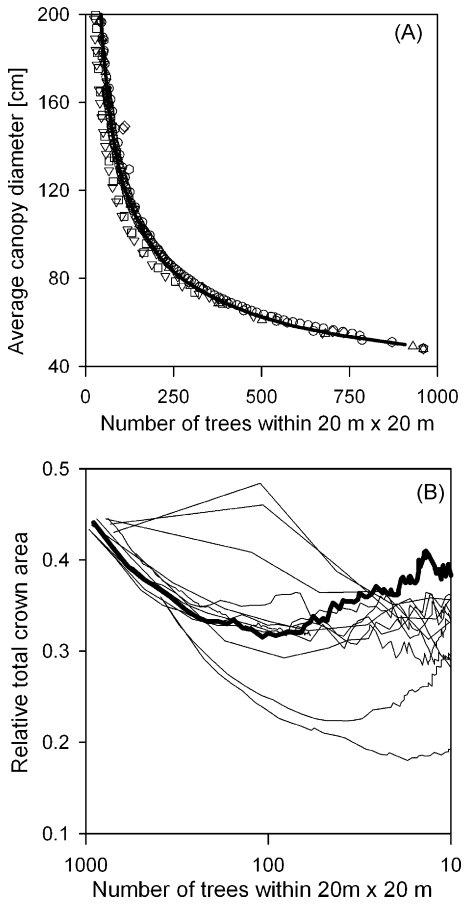

Fig. 4 – Self-thinning trajectories of the initial model. (A) Average tree size vs. tree density for the first 12 simulations of the sensitivity analysis (symbols) and under the standard parameters (cf. Table 1; bold line). Each symbol represents the situation for a given parameter set at a certain simulation time step. Simulations start in the lower right and follow the curve to the upper left. Every second time step is shown and thus 10 years have passed between two symbols of one simulation. Simulations were initialized with the size distribution of minimum-domain-areas (canopy sizes) observed in the field. These simulations follow a self-thinning line equivalent to a slope of −4/3 in the plant weight–density plane and a slope of −3/2 in the plant volume–density plane (Wiegand et al., unpublished). (B) Relative total crown area (summed crown areas divided by 20 m × 20 m) during the self-thinning process (quantified as tree density on a logarithmic scale) for the simulations shown in (A). Thin lines: sensitivity analysis, bold line: standard parameters.

Size inequality was typically explained at the 0.4 level only, presumably because some parameters interacted non-monotonically (cf. Section 5). The relative contribution of the parameters did depend on initial size–frequency distribution and time. When initially all plants were of equal size (I1), growth (θ, g) and local crowding (*ZOI_scale*) had a highly significant positive influence on size inequality within the first

10 time steps of the simulation, while later on only competition (*ZOI_scale* and *b*) was significant. This is because initially, fast growth (θ, *g*) sped up population dynamics and therefore developing size inequalities were apparent at earlier stages. In addition, large ZOIs led to interaction among many plants, which gave many opportunities for inequalities to develop. Later on, once some size inequality had developed, growth lost its role to the amount of interaction. Large ZOIs continued to contribute to more interactions in terms of the number of plants competing, and competitive asymmetry *b* increased existing inequality. Simulations initialized according to field tree sizes (I3) were different because comparatively high levels of size inequality were present right from the beginning of the simulations. Thus, competitive asymmetry *b* was highly significant throughout because it could fully draw on pre-existing size inequality. Surprisingly, *b* had, on average, a negative influence on size inequality. This is because of the increased mortality of smaller plants under strong size inequality, which caused a decrease in size inequality among living plants and thereby an increase in average plant size. Further to *b*, *ZOI_scale* contributed initially significantly and positively to size inequality; while fast growth (large θ) became important in later time steps because fast growth accelerated mortality and thereby significantly decreased size inequality (the influence of θ was negative).

5. Effect of local crowding and competitive asymmetry on size inequality

We now turn to the question of how local crowding (mediated by *ZOI_scale*) and competitive asymmetry *b* affect size inequality. The sensitivity analysis showed that *ZOI_scale* and *b* both contribute significantly to the generation of size inequality. *ZOI_scale* is the most important parameter for the creation of size inequalities, while competitive asymmetry *b* plays an important role in maintaining (or, via the mortality of smaller plants, reducing) existing size inequalities. Thus, spacing (*ZOI_scale*) and competitive asymmetry (*b*) are both key, but their relative importance is not known (cf. Weiner et al., 2001). Consequently, we further analyzed the simulations of the sensitivity analysis with respect to the influence of these two model parameters on the generation of size inequality (Appendix F).

As a measure of size inequality generated under a certain parameter set, we used the maximum value of the Gini coefficient (G_m) over the course of an entire simulation (200 time steps, calculated from the average over three runs, all 36 simulations in their entire length included). G_m is a useful measure because, during simulation runs initialized with plants of equal size, size inequality increases, reaches G_m, and decreases again when small trees die and large trees approach their maximum size (cf. Weiner and Whigham, 1988). In one case, growth was extremely slow ($g = 1.5$, $\theta = 0.011$) and, after 200 time steps, size inequality was still in its increasing phase. In this case, we approximated G_m with the Gini coefficient reached at the end of the simulation (time step 200).

An inspection of a three-dimensional plot of the data from the sensitivity analysis (I1; *ZOI_scale*, *b*, and G_m) indicated that *ZOI_scale* and G_m were linearly interrelated and *b* and G_m were

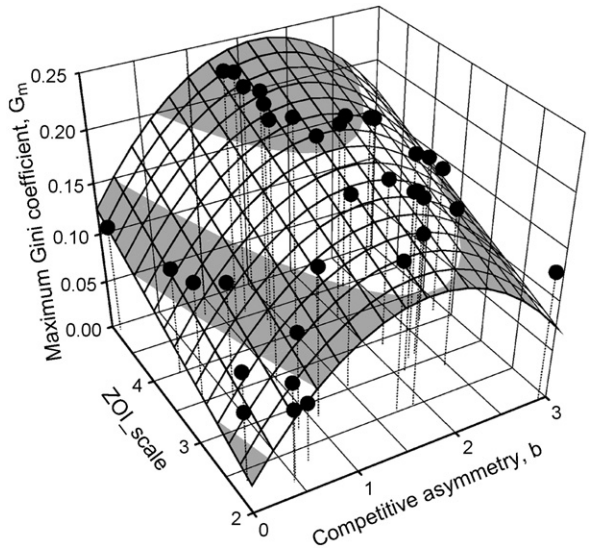

Fig. 5 – Maximum Gini coefficient reached over the course of a simulation (G_m) vs. *ZOI_scale* and competitive asymmetry *b*. All points shown are based on the sensitivity analysis initialized with plants of equal size (I1). The surface shows G_m as an interpolated function of *ZOI_scale* and *b* ($G_m = -0.0350 + 0.0320\,ZOI\_scale + 0.143b - 0.0426b^2$). The borders of gray shading on the surface are at $G_m = 0.05$, 0.10, 0.15 and 0.20.

interrelated by a quadratic polynomial (Fig. 5). Indeed, the regression $G_m = -0.0350 + 0.0320\,ZOI\_scale + 0.143b - 0.0426b^2$ fits the data well (adj. $r^2 = 0.70$; $P < 0.001$; $F = 27.8$; but *b* and b^2 have a Variance inflation factor ≈16). Intermediate values of *b* and intermediate to large values of *ZOI_scale* led to the greatest inequalities (Fig. 5). This is because large values of *ZOI_scale* mean that many plants interact and thus there is more opportunity for size inequalities to arise. Thus, the larger the *ZOI_scale*, the greater is the size inequality. However, if competitive asymmetry is very small, it does not matter how many plants interact because larger plants have no advantage over smaller plants. Thus, great size inequality could not arise under small competitive asymmetry even if *ZOI_scale* is large. For intermediate competitive asymmetries ($b \approx 1.5$), the increase in size inequality with increasing *ZOI_scale* was maximal because more and more plants interacted intensively. However, for greater competitive asymmetries, large plants suppressed their neighbors, had access to an increasing proportion of the resources, became even bigger and killed their small neighbors via death-by-contact. Consequently, there was high mortality among smaller plants and increasing size inequality was soon decreased due to mortality of small plants.

6. Attempt to parameterize model variant to an actual tree population

With the initial model (with four of five parameters estimated) and several biologically reasonable variants concerning growth rules and model initialization, our aim is now to find

a model variant that quantitatively reproduces patterns of size inequality under self-thinning observed for *A. reficiens* in Namibia. Following the POM idea, we require that the model variant and parameterization (with respect to the unknown value of *b*) reproduces, in addition to the self-thinning line (P0), two further patterns (P1 and P2) of the self-thinning process simultaneously. P1 is a realistic level of size inequality; henceforth measured in terms of the maximum value of the Gini coefficient over the course of an entire simulation (200 time steps, calculated from the average over three runs), G_m. In the field plots, which are 10 m × 10 m in size, the observed size inequality was on average $G = 0.284$ and ranged from $G = 0.209$ to 0.379. P2 requires that the average canopy diameter at which the maximum Gini coefficient is exhibited in the model (dG_m) is realistic. In the field plots, the canopy diameter averaged across plots at 73 cm and ranged from 48 cm to 91 cm. P2 is a secondary prediction, i.e. has not been used for model development. Thus, fulfillment of P2 can be regarded as model validation (Wiegand et al., 2003).

The sensitivity analysis showed that all processes included in our initial model are essential to the generation of size inequality. Consequently, we examine first whether the initial model already generates realistic levels of size inequality (P1) under the full range of parameters given in Table 1. If not, additional features need to be added to the initial model. Candidates for such additional features are the stochastic growth scenarios G2–G4 given in Section 3. Condition for the best-fit model variant is that it satisfies both patterns, P1 and P2. Note that variations G1–G4 of the initial model will in any case reproduce the self-thinning line P0 (cf. Wiegand et al., unpublished).

When comparing these patterns, we must take into account the different nature of field and simulated data. The simulation results are extremes of time series while the field data represent snapshots. Thus, it is possible that the maximum size inequality in the field is underestimated by our data. Also, the minimum-domain-diameter at which size inequality is maximal may both be smaller or larger than those currently observed in the field. Obviously, there is considerable variation in the size inequality observed in the field but no relationship between size inequality and minimum-domain-diameter (see Fig. 6 or Wiegand et al., 2005). From this, we derive two interpretations: (1) spatial habitat heterogeneity has a noticeable influence on size inequality and therefore explains the great degree of variation. Given that the simulation model excludes spatial habitat heterogeneities, we cannot expect to reproduce with the model the maximum size inequality observed in the field. Rather, model predictions are expected to be at the lower end of the field values. (2) The simplest explanation for the lack of trend in the inequality–size relationship is that field populations are near their maximum size inequality. Based on these considerations, we decided not to compare field and model data via statistical tests but devised the following pattern fulfillment criteria: model variants are considered to meet the criterion of realistic size inequality (P1) if they fall between the minimum (0.209) and average (0.284) size inequality observed in the field plots (cf. interpretation (1)). The criterion of realistic tree size at maximal size inequality (P2) is based on the range of minimum-domain-areas observed in the field (minimum: 47.96 cm, maximum: 99.32 cm, range: 51.37 cm). A model variant is considered to meet P2 if the minimum-domain-area under this scenario is within the minimum minus a buffer of 50% of the range and the maximum minimum-domain-area observed in the field plus a buffer of 50% of the range (cf. interpretation (2)). Our aim is to find model variants that concurrently meet patterns P1 and P2 (see box in Fig. 6).

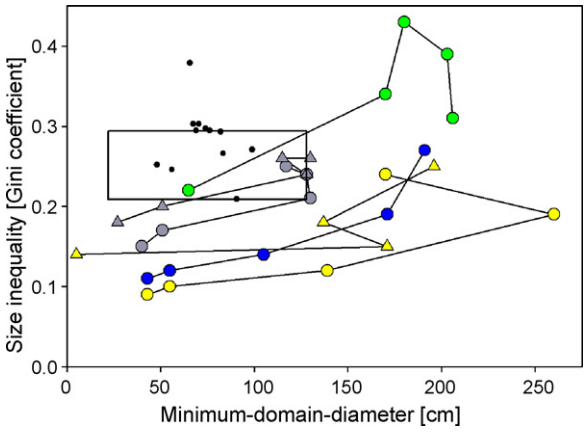

Fig. 6 – Maximum size inequality (Gini coefficient) reached over the course of a simulation P1 vs. the average minimum-domain-diameter under which this maximum inequality was reached under different growth scenarios (as in Table 2; colored symbols) and for several competitive asymmetries *b*. Symbol shape represents initial tree size–frequency distribution (*circles*: I1, equal size; *triangles*: I2, normally distributed sizes). Symbol color represents growth scenario (*yellow*: G1, initial model; *green*: G2, growth rates different among plants; *blue*: G3, normally distributed growth rates; *gray*: G4 double stochastic growth including increase and decrease in plant size). Competitive asymmetries are increasing from left to right following the black lines ($b = 0.0, 0.3, 0.5, 0.7, 1.0$). Black dots represent the Gini coefficient vs. the average minimum-domain-area in 12 field plots described in Wiegand et al. (2005). The rectangle represents the area within which model simulations fulfill patterns P1 and P2 and has been constructed based on the different nature of the model and field data.

6.1. *Levels of size inequality in field populations and under the initial model*

Here, we check if our initial model creates realistic levels of size inequality in which case the initial model could serve as a successfully validated model of self-thinning under size inequality of *A. reficiens* in Namibia. However, we find that, maximum inequalities during the course of the model simulations initialized with trees of equal size (I1) tended to be much lower than those observed in the field, i.e. the initial model does not meet P1 (model results of sensitivity analysis: average $G_m = 0.162$, range: 0.056–0.274, simulated area: 20 m × 20 m). Also, the mean canopy diameter at which the maximum Gini coefficient was observed in the model (dG_m) was high compared to the size of the trees that had been investigated in the field, i.e. the initial model does not meet P2 either (model:

Table 2 – Size inequality (Gini coefficient) at an average tree size of about 73 cm under different growth scenarios, i.e. P2

b	I1–G1	I2–G1	I1–G2*	I1–G3*	I1–G4*	I2–G4*
0.0	0.08	0.09	**0.22**	0.10	0.12	0.14
0.3	0.10	0.12	**0.29**	0.12	0.17	0.19
0.5	0.12	0.14	**0.33**	0.14	0.20	**0.23**
0.7	0.13	0.16	**0.34**	0.16	**0.22**	**0.24**
1.0	0.18	0.20	**0.30**	0.21	**0.23**	**0.25**

Notes: The aim of this table is to find model scenarios where size inequality has similar levels to size inequality in the field ($G = 0.28$; 95% confidence interval = [0.22, 0.33]; agreement indicated in bold), when model populations have the same average tree size as field populations (a maximum canopy size of 73 cm). All simulations were run under standard parameters given in Table 1 except for the competitive asymmetry b, which was varied from 0.0 to 1.0. Simulations were initialized with 1000 plants distributed in an area of 20 m × 20 m after Matérn (1960). Initial plant size was either equal (5 cm, I1) or normally distributed (mean: 5 cm, S.D.: 1.25 cm, I2). Simulations consisted of 3 or 10 (indicated with *) simulation runs. All values are averages across all trees and a certain year (chosen to match average tree size of 73 cm as closely as possible) of all simulation runs. G1: initial model; G2: growth rate different among plants but constant through time; G3: stochastic growth rate following a normal distribution with mean g; G4: double stochastic growth process accounting for the possibility of both increase (95% probability) and decrease (5%) in plant size by $-g$ and $2.105g$, respectively. Growth rates were drawn from two normal distributions with the respective means and standard deviation $0.25g$. The minimum-domain-diameter of *A. reficiens* was approximated by the maximum canopy diameter.

average $dG_m = 134$ cm, range: 41–285). Thus, competition as described in our ZOI model was not sufficient to generate realistic size inequality from initially equal-sized seedlings.

6.2. *Generation of realistic size inequalities*

To investigate the influence of stochastic variabilities in growth on size inequality, we conducted a series of six simulation experiments for a range of competitive asymmetries (Fig. 6; Table 2) and using the standard values for the remaining parameters (Table 1). The scenarios differ in the initial size distribution (I1 and I2) and in the stochastic variability of the growth rate g (G1–G4).

Under the two reference cases corresponding to the initial model (I1–G1, I2–G1), size inequality can reach values similar to field observations, i.e. approximate pattern P1 when b is sufficiently large. This is especially true in scenario I2–G1 due to the size inequalities present in the initial size distribution (note that this case (I2) was not investigated in the previous section). However, these values are reached only at average tree sizes way beyond the average size of 73 cm investigated in the field (Fig. 6), a size at which size inequality is still below 0.2 in these simulations (P2; Table 2). Thus, we confirm the conclusion from the previous section that the initial model does not meet pattern P2.

Under growth rates variable across trees but constant over time (I1–G2), size inequality is realistic at low values of competitive asymmetry b (meeting P1) but too great for larger size inequalities (not meeting P1). Positive growth rates changing from year to year (I1–G3) are not able to create realistic inequality from initially equal-sized trees, i.e. fail to meet P1. However, if stochasticity includes both increases and decreases in plant growth (I1–G4), maximum inequality is similar to the average field value of 0.28 at $b = 0.7$ and 1.0 (meeting P1) and size inequality at 73 cm average size equals 0.22 (Table 2). These values increase somewhat when size inequality in the initial size distribution is included (I2–G4; Fig. 6; Table 2). Irrespective of the initial tree size distribution (I1 or I2), simulations under G4 reach maximum size inequality at realistic average tree sizes (Fig. 6), i.e. meet P2.

6.3. *Selecting the model variant that best reproduces size inequality*

In summary, among the factors investigated here, tree-specific, constant growth rates (G2) have the greatest potential to generate size inequality (meet P1). However, apart from genetic differences, it seems unrealistic that such differences in growth rates among plants persist for many years (for a different opinion, see Turner and Rabinowitz, 1983). The scenario with the second highest size inequality included variable initial sizes and variable (both positive and negative) growth. This scenario I2–G4 also reaches maximum size inequality at reasonable average tree sizes (meets P2) and is biologically plausible. Therefore, among the models tested, the model with I2–G4 is most suitable as "best-fit" model of size inequality for our study site. Nevertheless, the size inequality under scenario I2–G4 is still somewhat below the size inequality found in the field, meaning that we were not able to successfully validate our model at our study site. Though tested as a separate hypothesis, it is likely that growth regimes G2 (correlation of growth rates through time) and G4 (stochastic increase and decrease) are not mutually exclusive. Future field and modeling research should test the hypothesis that a combination of G2 and G4 drives size inequality. From the current study, we can already derive the conclusion that size inequality is driven not only by competitive asymmetry and the size of the ZOI but a full range of details of plant growth is responsible for size inequalities observed in the field.

6.3.1. *Fixing a standard value for competitive asymmetry*

We have seen in Section 5 that intermediate degrees of competitive asymmetry (b) lead to the greatest inequalities (Fig. 5) and that the size at which the maximum inequality is reached increases with increasing b. This means when choosing b, a small to intermediate value should be chosen in order to reach relatively high inequalities for trees as young (small) as possible. Based on our parsimonious model (scenario I2–G4 in Table 2), a value of $b = 1.0$ seems appropriate. However, further field and modeling research will be needed for a good estimate of b.

7. Discussion

7.1. *Major model assumptions*

A challenge in modeling is to find a good balance between realism and simplicity. Most published self-thinning models

aim for simplicity and have been found to rely on biologically unreasonable representations of competition (Reynolds and Ford, 2005). Despite a great number of simplifications and in contrast to published self-thinning models as reviewed in Reynolds and Ford (2005), our model does (1) not rely on representing the population by the mean plant, (2) not assume a constant total minimum-domain-area (representing projected crown area; Fig. 4B), (3) explicitly consider competitive hierarchy developing from differential access to resources, and (4) allow for differences in initial stand conditions to affect the process of self-thinning (e.g., Appendix E: Fig. E.1). This comparatively high level of realism was facilitated by a spatially explicit, individual-based modeling approach (Grimm et al., 2005). However, one may criticize that our model ignores morphological plasticity in response to competition (e.g. Mohler et al., 1978; e.g. Gilbert et al., 2001; Stoll et al., 2002). Our model development was guided by the ecology of *A. reficiens* in arid savanna. This species mainly competes for belowground resources in a shallow soil layer, which facilitated a two-dimensional modeling approach that eliminated plasticity in tree height. Brisson and Reynolds (1997) observed plasticity in root growth in *Larrea tridentata* in a winter rain desert. However, the spatial root distribution of *A. mellifera* is not affected by competitors (Ward and Wiegand, personal observation in the Kalahari thornveld, South Africa). Thus, we did not include plasticity in root growth for two reasons: (1) simplicity and (2) our study species and area are ecologically more similar to the *A. mellifera*-observation.

We believe that in an equivalent model that includes height plasticity, the relative competitive hierarchy would have remained unaltered and thus would have had a quantitative but no qualitative effect on our results. If data on tree allometry during self-thinning are available, the effect of plasticity in height growth on the biomass/volume–tree density relationship can be estimated by transforming minimum-domain-area to biomass or volume accordingly.

7.2. Self-thinning

Wiegand et al. (unpublished) developed a parsimonious model of self-thinning with a single condition that the self-thinning line is reproduced. Starting from the same initial model as used in the present paper, it was possible to cut down the initial model dramatically to a model lacking a zone of influence and thereby details on inter-tree competition other than death-by-contact. This model reduces self-thinning to a pure geometric process, i.e., packing circles in two-dimensional space conditional upon the spatial distribution of seedlings at the time of establishment (cf. White, 1981). In this paper, we advance from pure geometry to an understanding of the mechanisms of self-thinning by looking for a model that reproduces several patterns of the self-thinning process simultaneously (self-thinning line, the degree of size inequality, and the average size of the population at which a certain degree of size inequality is reached). Due to the two additional patterns, this model of self-thinning under size inequality is a much more realistic representation of the processes driving tree population dynamics. Adler (1996) reproduced the self-thinning rule using a dynamic model including size inequality and local resource competition but excluding explicit mortality. Due to the lack of explicit mortality, Adler's (1996) model establishes only an indirect connection between local plant competition and self-thinning because it relies on average ensemble properties instead of modeling mortality at the level of the individual. However, in the present paper, we could establish the direct link between local competition that drives mortality at the level of the individual and self-thinning.

Interestingly, the model variant that best meets the field patterns contains virtually all factors hypothesized to cause size inequality: spatial pattern, competitive asymmetry, variation in post-emergence size, and stochastic growth variation including sporadic decreases in plant size and, possibly, spatial heterogeneity (not investigated here). We did not expect the more complex model variants to yield better model fits because all model variants were developed and parameterized *a priori* (with the exception of the degree of size asymmetry). Thus, our results show that self-thinning is a complex process and that true understanding of self-thinning requires investigation of multiple patterns.

7.3. Size inequality

Most modeling studies on the generation of size inequality focus on populations that are not crowded. Studies on size inequality in uncrowded populations observe increasing size variation over time (e.g., reviewed in Wyszomirski, 1986). However, in self-thinning populations in the field, the smallest individuals have the lowest rate of survivorship (e.g., Ford, 1975; Kenkel et al., 1997). Thus, mortality counteracts the increasing size inequality caused by competition and has been observed to cause a net-decline in size inequality (Weiner and Whigham, 1988). However, beyond mortality, the same factors should cause size inequality in both uncrowded and crowded conditions.

The factors causing size inequality are a matter of debate leading to a series of modeling studies. Several models have shown that variation in local crowding is sufficient to increase size variability (Huston, 1986; Miller and Weiner, 1989; Bonan, 1991). As a consequence of local variation in the size, proximity, and number of neighbors, different plants have access to different quantities of resources and thus size inequality is augmented via differences in their growth rate. However, this phenomenon cannot be sufficient to explain the degree of size inequality observed in nature because size variation is commonly observed in forest plantations with regularly spaced individuals of initially nearly equal size (e.g., Harms et al., 1994). Alternatively, size variability may increase because of asymmetry in competition between individuals, meaning that larger individuals obtain a disproportionate share of the resources for their relative size (Weiner and Thomas, 1986; Weiner, 1990). Thus, initially small differences in plant size will be increased over time and self-thinning will eventually reduce inequality.

Our model indicates that both local crowding and asymmetric competition generate size inequalities (see also Weiner et al., 2001), and their relative importance may vary greatly. It is difficult to separate their relative importance in the field because they both interact and because a general evaluation would require one to understand susceptibility to differences in spatial pattern (*ZOI_scale*) and the mode of competition (*b*)

for a variety of plants. In the modeling literature, the effect of variation in local crowding is tested by using different spatial patterns (hexagonal, random; e.g., Bonan, 1988; Miller and Weiner, 1989; Weiner et al., 2001). Certainly, for plant cultivation, it may be important to conduct such simulations in order to develop planting patterns that minimize size variation. However, from an ecological point of view, it is an indirect way of analyzing the importance of spacing. The relative importance of spacing depends on the spatial range over which plants are interacting with neighbors. By changing *ZOI_scale*, we have changed this range and were able to relate it to size inequality. Specifically, *ZOI_scale* can have a significant effect on size variation and thus determine whether spatial pattern or the competitive mode is more important. We agree with Weiner et al. (2001) who state "Overall, two-dimensional ZOI studies to date have explored very small regions of the biologically relevant parameter space [...]. Advances in computing technology [...] allow us to make more informative simulation studies". In this spirit, our answer to the problem of not knowing the real-world values of competitive asymmetry and *ZOI_scale* was to conduct a global sensitivity analysis in which both have been varied independently over a range of values. Indeed, we found a great deal of interaction between competitive asymmetry and *ZOI_scale* as they determine size inequality. Thus, assuming an arbitrary, constant relation between ZOI and plant size and investigating only extreme cases of competitive asymmetry, as frequently done in the literature, would have led to spurious results. For example, investigating exclusively a *ZOI_scale* of, say, 2.0 and extreme competitive asymmetries b of, say, 0.0 and 3.0 would have led to the conclusion that competitive asymmetry has a moderately positive influence on size inequality (from $G_m \approx 0.0$ to ≈ 0.1; Fig. 5), overlooking the much greater size inequality $G_m \approx 0.25$ at the more realistic parameter values *ZOI_scale* = 3.5 and $b = 1.0$. In other words, model results showing that extreme asymmetry can override effects of spatial distribution (in our case *ZOI_scale*) may well be meaningless if real plants never exhibit such extreme asymmetry. As a consequence, the relative importance of crowding is likely to be species specific as it depends on the size of the area within which plants compete with neighbors, a species-specific property (cf. Bella, 1971).

Spatial pattern and the mode of competition are not the only factors contributing to the generation of size inequalities. One further factor is plant density (e.g., Bonan, 1991; Weiner et al., 2001), which was not investigated by us because of our special interest in crowded populations. Other factors we have examined are variation in the initial size distribution, stochastic variation in the inherent growth rate among plants, and stochastic between-year variation in the growth rate of all plants (all reviewed in Benjamin and Hardwick, 1986). These factors not only contributed to size inequality but also were necessary to produce size variation similar to the variation observed in the field. Furthermore, our simulations show that their influence on size inequality can be similar in magnitude to the influence of competitive asymmetry (Fig. 6; Table 2). However, suggestions that variation in growth rates during the exponential growth phase of plants could explain plant size variation (Turner and Rabinowitz, 1983), seem unrealistic for long-lived plants. Our point of view is that a series of factors, and interactions among them, significantly influence plant sizes.

7.4. *Pattern-oriented modeling POM*

In this study, we applied POM with different degrees of success. Based on literature and own field data, we successfully designed the structure of the initial model so that both the self-thinning line and size inequality emerged. We were also able to better understand the two leading hypotheses for generation of size inequality and pinpoint that instead of being mutually exclusive, they interact to generate size inequality. One way to look at Fig. 5 is that different combinations of local crowding and competitive asymmetry may lead to the same level of size inequality. Thus, the degree of size inequality alone cannot be used to infer and quantify the underlying mechanisms. This will frequently be the case due to non-linearities and it emphasizes the importance of observing multiple patterns. We used multiple patterns to infer the mechanisms causing size inequality at our study site. However, our best-fit model variant still underestimates actual size inequality, suggesting yet another mechanism, not explored in this study. A common feature of the variations to the initial model (explored and not explored) is stochasticity. Thus, the next logical step would be to collect more field data that serve to quantify the degree of stochasticity in nature and thereafter attempt a second modeling cycle. Thus, this study shows that POM has its merits and limitations. Ultimately, knowledge and understanding are fleeting ideals that we must approach in small steps. POM facilitates but does not relieve us from several cycles of fieldwork and modeling.

8. Conclusions

The self-thinning line was first discovered almost a century ago (Frothingham, 1914) and has received continuous attention since Yoda et al. (1963) and White and Harper (1970). We propose that the key to understanding this aggregated pattern is to include co-occurring patterns such as size inequality in the investigations. As shown in this paper, reproducing the self-thinning line under size inequality is far more difficult than reproducing self-thinning alone and helps to understand the underlying processes. Our modeling study suggests that these processes are inter-tree competition along with stochasticity in both initial tree sizes and plant growth and thus highlights the importance of stochasticity in ecological processes.

Acknowledgements

We thank Fred Adler, Helene Muller-Landau, and especially Thorsten Wiegand for inspiring discussions and comments that improved the presentation of our results. We also thank the anonymous reviewers for helpful comments. K. Wiegand gratefully acknowledges financial support by the "Gemeinsames Hochschulsonderprogramm III von Bund und Ländern" of the German Academic Exchange Service (DAAD), the Andrew W. Mellon Foundation (grant to S.A. Levin), the Blaustein Center for Scientific Cooperation of the Jacob

Blaustein Institute for Desert Research, partial funding by BIOLOG program of the German Ministry of Science (BMBF; grant to V. Wolters and W. Köhler), the Volkswagen foundation, the German Science Foundation (DFG), and a DFG travel grant. This is publication no. 578 of the Mitrani Department for Desert Ecology and publication no. 235 of the Ramon Science Center.

Appendices A–F. Supplementary data

Supplementary data associated with this article can be found, in the online version, at doi:10.1016/j.ecolmodel.2007.08.027.

REFERENCES

Adler, F.R., 1996. A model of self-thinning through local competition. PNAS 93, 9980–9984.
Aikman, D.P., Watkinson, A.R., 1980. A model for growth and self-thinning in even-aged monocultures of plants. Ann. Bot. 45, 419–427.
Bella, I.E., 1971. A new competition model for individual trees. Forest Sci. 17, 364–372.
Benjamin, L.R., Hardwick, R.C., 1986. Sources of variation and measures of variability in even-aged stands of plants. Ann. Bot. 58, 757–778.
Bonan, G.B., 1988. The size structure of theoretical plant populations: spatial patterns and neighborhood effects. Ecology 69, 1721–1730.
Bonan, G.B., 1991. Density effects on the size structure of annual plant populations: an indication of neighborhood competition. Ann. Bot. 68, 341–347.
Brisson, J., Reynolds, J.F., 1997. Effects of compensatory growth on population processes: a simulation study. Ecology 78, 2378–2384.
Cannell, M.G.R., Rothery, P., Ford, E.D., 1984. Competition within stands of *Pinus sitchensis* and *Pinus contorta*. Ann. Bot. 53, 349–362.
Carr, J.D., 1976. The South African Acacias. Conservation Press (Pty) Ltd., Johannesburg, London, Manzini.
Cody, M.L., 2000. Slow-motion population dynamics in Mojave Desert perennial plants. J. Veg. Sci. 11, 351–358.
Coughenour, M.B., Ellis, J.E., Popp, R.G., 1990. Morphometric relationships and developmental patterns of *Acacia tortilis* and *Acacia reficiens* in southern Turkana, Kenya. Bull. Torrey. Bot. Club. 117, 8–17.
Davie, T.J.A., 1999. A numerical model to quantify the growth of a canopy for a forest hydrology model. Appl. Geogr. 19, 45–67.
Enquist, B.J., Niklas, K.J., 2001. Invariant scaling relations across tree-dominated communities. Nature 410, 655–660.
Enquist, B.J., Brown, J.H., West, G.B., 1998. Allometric scaling of plant energetics and population density. Nature 395, 163–165.
Ford, E.D., 1975. Competition and stand structure in some even-aged plant monocultures. J. Ecol. 63, 311–333.
Frothingham, E.H., 1914. White pine under forest management. U.S. Department of Agriculture Bulletin 13.
Gilbert, I.R., Jarvis, P.G., Smith, H., 2001. Proximity signal and shade avoidance differences between early and late sucessional trees. Nature 411, 792–795.
Gilpin, M.E., Case, T.J., Ayala, F.J., 1976. Theta-selection. Math. Biosci. 32, 131–139.
Glasser, G.J., 1962. Variance formulas for the mean difference and coefficient of concentration. J. Am. Stat. Assoc. 57, 648–654.
Goldberg, D.E., Turner, R.M., 1986. Vegetation change and plant demography in permanent plots in the Sonoran Desert. Ecology 67, 695–712.
Grimm, V., Revilla, E., Berger, U., Jeltsch, F., Mooij, W.M., Railsback, S.F., Thulke, H.-H., Weiner, J., Wiegand, T., DeAngelis, D.L., 2005. Pattern-oriented modeling of agent-based complex systems: lessons from ecology. Science 310, 987–991.
Hamilton, N.R.S., Matthew, C., Lemaire, G., 1995. In defense of the −3/2 boundary rule—a reevaluation of self-thinning: concepts and status. Ann. Bot. 76, 569–577.
Hara, T., 1985. A model for mortality in a self-thinning plant population. Ann. Bot. 55, 667–674.
Hara, T., 1988. Dynamics of size structure in plant populations. Trends Ecol. Evol. 3, 129–133.
Harms, W.R., DeBell, D.S., Whitesell, C.D., 1994. Stand and tree characteristics and stockability in *Pinus taeda* plantations in Hawaii and South Carolina. Can. J. For. Res. 24, 511–521.
Higgins, S.I., Bond, W.J., Trollope, S.W., 2000. Fire, resprouting and variability: a recipe for grass-tree coexistence in savannna. J. Ecol. 88, 213–229.
Huston, M., 1986. Size bimodality in plant populations: an alternative hypothesis. Ecology 67, 265–269.
Kendall, B.E., Briggs, C.J., Murdoch, W.W., Turchin, P., Ellner, S.P., McCauley, E., Nisbet, R.M., Wood, S.N., 1999. Why do populations cycle? A synthesis of statistical and mechanistic modeling approaches. Ecology 80, 1789–1805.
Kenkel, N.C., Hendrie, M.L., Bella, I.E., 1997. A long-term study of *Pinus banksiana* population dynamics. J. Veg. Sci. 8, 241–254.
Leps, J., Kindlman, P., 1987. Models of the development of spatial pattern of an even-aged plant population over time. Ecol. Modell. 39, 45–57.
Levin, S.A., 1992. The problem of pattern and scale in ecology. Ecology 73, 1943–1967.
Luxmoore, R.J., King, A.W., Tharp, M.L., 1991. Approaches to scaling up physiologically based soil plant-models in space and time. Tree Physiol. 9, 281–292.
Matérn, B., 1960. Spatial variation. Meddelanden fran Statens Skogsforskningsinstitut Stockholm 49, 1–177.
McKay, M.D., Beckman, R.J., Conover, W.J., 2000. A comparison of three methods for selecting values of input variables in the analysis of output from a computer code. Technometrics 42, 55–61.
Miller, R.E., Huenneke, L.F., 2000. Demographic variation in a desert shrub, *Larrea tridentata*, in response to a thinning treatment. J. Arid. Environ. 45, 315–323.
Miller, T.E., Weiner, J., 1989. Local density variation may mimic effects of asymmetric competition on plant size variability. Ecology 70, 1188–1191.
Milton, S.J., 1995. Spatial and temporal patterns in the emergence and survival of seedlings in arid Karoo shrubland. J. Appl. Ecol. 32, 145–156.
Mohler, C.L., Marks, P.L., Sprugel, D.G., 1978. Stand structure and allometry of trees during self-thinning of pure stands. J. Ecol. 66, 599–614.
Niklas, K.J., 1994. Plant Allometry: The Scaling of Form and Process. The University of Chicago Press, Chicago and London, 395 pp.
Palgrave, K.C., 1977. Trees of Southern Africa. C. Struik Publishers, Cape Town.
Porco, T.C., Blower, S.M., 1998. Quantifying the intrinsic transmission dynamics of tuberculosis. Theor. Popul. Biol. 54, 117–132.
Reynolds, J.H., Ford, E.D., 1999. Multi-criteria assessment of ecological process models. Ecology 83, 538–553.
Reynolds, J.H., Ford, E.D., 2005. Improving competition representation in theoretical models of self-thinning: a critical review. J. Ecol. 93, 362–372.

Richards, F.J., 1959. A flexible growth function for empirical use. J. Exp. Bot. 10, 290–300.
Ross, J.H., 1979. A conspectus of the African *Acacia* species. Mem. Bot. Surv. S. Afr. 44, 1–155.
Slatkin, M., Anderson, D.J., 1984. A model of competition for space. Ecology 65, 1840–1845.
Smith, T.M., Goodman, P.S., 1986. The effect of competition on the structure and dynamics of *Acacia* savannas in Southern Africa. J. Ecol. 74, 1013–1044.
Stoll, P., Weiner, J., Muller-Landau, H., Müller, E., Hara, T., 2002. Size symmetry of competition alters biomass–density relationships. Proc. R. Soc. Lond. B 269, 2191–2195.
Turner, M.D., Rabinowitz, D., 1983. Factors affecting frequency distributions of plant mass: the absence of dominance and suppression in competing monocultures of *Festuca paradoxa*. Ecology 64, 469–475.
Van der Merwe, J.H. (Ed.), 1983. National Atlas of South West Africa. National Book Printers, Cape Town, South Africa.
Ward, D., Rohner, C., 1997. Anthropogenic causes of high mortality and low recruitment in three *Acacia* tree species in the Negev desert, Israel. Biodivers. Conserv. 6, 877–893.
Ward, D., Saltz, D., Ngairorue, B.T., 2004. Spatio-temporal rainfall variation and stock management in arid Namibia. J. Range Manage. 57, 130–140.
Weiner, J., 1990. Asymmetric competition in plant populations. Trends Ecol. Evol. 5, 360–364.
Weiner, J., Solbrig, O.T., 1984. The meaning and measurement of size hierarchies in plant populations. Oecologia (Berlin) 61, 334–336.
Weiner, J., Thomas, S.C., 1986. Size variability and competition in plant monocultures. Oikos 47, 211–222.
Weiner, J., Whigham, D., 1988. Size inquality and self-thinning in wild-rice (*Zizania aquatica*). Am. J. Bot. 75, 445–448.
Weiner, J., Stoll, P., Muller-Landau, H., Jasentuliyana, A., 2001. The effects of density, spatial pattern, and competitive symmetry on size variation in simulated plant populations. Am. Nat. 158, 438–450.
Westoby, M., 1984. The self-thinning rule. Adv. Ecol. Res. 14, 167–225.
White, J., 1981. The allometric interpretation of the self-thinning rule. J. Theor. Biol. 89, 475–500.
White, J., Harper, J.L., 1970. Correlated changes in plant size and number in plant populations. J. Ecol. 58, 467–485.
Wiegand, K., Ward, D., Saltz, D., 2005. Multi-scale patterns in an arid savanna with a single soil layer. J. Veg. Sci. 16, 311–320.
Wiegand, K., Saltz, D., Ward, D., 2006. A patch dynamics approach to savanna dynamics and woody plant encroachment—insights from an arid savanna. Persp. Plant Ecol. Evol. Sys. 7, 229–242.
Wiegand, K., Saltz, D., Ward, D., Levin, S.A. Self-thinning and tree dynamics in arid savannas: a zone-of-influence model, unpublished.
Wiegand, T., Jeltsch, F., Hanski, I., Grimm, V., 2003. Using pattern-oriented modeling for revealing hidden information: a key for reconciling ecological theory and application. Oikos 100, 209–222.
Wiens, J.A., 1989. Spatial scaling in ecology. Funct. Ecol. 3, 385–397.
Wood, S.N., 2001. Partially specified ecological models. Ecol. Monogr. 71, 1–25.
Wyszomirski, T., 1986. Growth, competition and skewness in a population of one-dimensional individuals. Ecol. Pol. 34, 615–641.
Wyszomirski, T., 1992. Detecting and displaying size bimodality: kurtosis, skewness, and bimodalizable distributions. J. Theor. Biol. 158, 109–128.
Yoda, K., Kira, T., Ogawa, H., Hozumi, K., 1963. Intraspecific competition among higher plants. XI. Self thinning in overcrowded pure stands under cultivated and natural conditions. J. Biol. Osaka City Univ. 14, 107–129.